OPEN ACCESS Freely available online

Journal of Geography and Natural Disasters

ISSN: 2167-0587

Research Article

Environmental Impact of Recent Volcanic Eruption from Mt. Mayon over South-East Asia

Arpit Tiwari*, Siddhartha Singh, Soni V.K, Ravi Ranjan Kumar

India Meteorological Department, Environment Monitoring and Research Center, New Delhi, India

ABSTRACT

Volcanoes are the mountains that erupt metallic compounds in the form of Lava, dust and gases vulnerable to the environment. These erupted gases affect the physical and chemical characteristics of Aerosol particles present in the atmosphere by absorbing the incoming radiation from the sun. This process has a huge contribution towards instability of the Heat budget of the Earth and leads to global warming and climate change. Compounds of sulfur e.g. ($H2S$, $C2S$, $SO4$) erupted from a volcano have severe effect on climate by scattering the incoming sunlight back to the space and leads to increased cooling rate of the earth surface. In this paper; short term and immediate effects of volcanic eruption from Mayon volcano have been discussed. The recent eruption of Mt. Mayon at Albay, Philippines on 29th Jan 2018 affected huge vegetation and environmental impacts of this eruption are found up to Brunei and Sarawak province of Malaysia. The study revealed that outbound airmass patternss from Mt. Mayon had Southwest direction that carried Sulfur dioxide and ash plumes till Malaysia. The case study shows huge vegetation loss and sudden rise in SO2 concentration over Sarawak from 1st Feb 2018 to 4th Feb 2018.

Keywords: aerosols; radiative effect; extinction; global dimming

INTRODUCTION

Volcanic eruptions are listed as severe natural hazard that affect the Earth system by producing Lava to the earth surface along with aerosol particles and gases to the atmosphere [1,2]. Lava or molten rock is referred as emerging liquid having very high temperatures of molten rocks ranging from about 700 ℃ to 1,200 °C onto Earth's surface. The term lava is also used for the solidified rock formed by the cooling of a molten lava flow. The higher the lava's silica content, the higher its viscosity [3]. Volcanic eruptions can disperse huge amount of chemically and micro physically active gases and solid aerosol particles into the stratosphere, which disturb the stratospheric chemical equilibrium. Some volcanic eruptions are explosive as compared to others [4]. The explosivity of a volcanic eruption depends on the composition of the magma. If magma inside the volcano is thin, gases can escape easily from it. This type of magma erupts smoothly out of the volcano. Hawaiian volcanoes are a good example of such eruptions. If the magma inside the volcano is thick and sticky, gases cannot escape easily and explosion occurs by building up the pressure until the gases escape violently. Mount St. Helens at Washington is a good example of such eruption [5]. In this type of eruption, the magma blasts into the air and breaks into pieces called tephra. Tephra can range in size from few nanometers to house-size boulders. Explosive volcanic eruptions can be dangerous enough to affect plants, animals, and humans [6]. Volcanic magma flows down destroying almost everything in their path. Volcanic Ash erupted into the atmosphere falls back to Earth like powdery snow and this thick ash can suffocate plants and living species. When hot volcanic materials mix with water from streams or melted snow and ice, mudflows form that can burry entire communities located near erupting volcanoes (USGS). Mayon is an active stratovolcano located at 13.2548° N, 123.6861° E in the province of Albay in Bicol Region, on the large island of Luzon in the Philippines [7-9]. The location of the volcano is described in Figure 1 below.

Correspondence to: Arpit Tiwari, India Meteorological Department, Environment Monitoring and Research Center, New Delhi, India, Tel: 91-880-087-5754, E-mail: rpttwr22@gmail.com

Received: December 16, 2020, **Accepted:** December 31, 2020, **Published:** January 07, 2021

Citation: Tiwari A, Singh S, Soni VK, Kumar RR (2021) Environmental Impact of Recent Volcanic Eruption from Mt. Mayon Over 1 South-East Asia. J Geogr Nat Disast 10:4.

Figure 1: Mt. Mayon

The atmosphere is comprised of several aerosol particles that can be in solid or liquid state. Glasow et al. stated that these gases and compounds react with each other and form several other compounds that can be of atmospheric relevance [10]. Atmospheric dynamics provides a medium to transport gases and particles over large distances. The troposphere is distributed from earth surface to about 10 km where most of the weather events occur. The topmost layer of the troposphere is called Tropopause which is capped by a very strong temperature inversion. Stratosphere takes place after the tropopause up to 50 Kms. A very strong, explosive volcanic eruption can penetrate the tropopause [11]. Dispersion and deposition of the pollutants is strongly connected to the Planetary Boundary Layer (PBL). PBL is a dense atmospheric pressure layer that shifts downward or upward depending upon the inversion. In winter season; PBL shifts downward and prevents the dispersion of pollutants emitted from the surface sources [12]. Vertical transport of pollutants from the earth surface becomes slow when the air reaches the free troposphere [13]. It is difficult to identify a small eruption using ground based sources therefore measuring volcanic emissions from space-born platforms is now a rapidly evolving field. These measurements allow global coverage with resolution upto few meters. Therefore; even a small volcanic eruption can be detected in extremely remote areas [14]. The traditional volcanic eruptions monitoring was a difficult task because earlier satellites were able to provide resolution up to few Kilometers only. The limitations of these satellites were to monitor small eruption [15]. Sentinel 2 mission is a revolutionary platform that provides resolution up to 10 Meters, 20 Meters and 60 Meters that can detect even small eruption also [16]. Sentinel-2 satellite is the combination of two identical sentinel satellites named as S2A and S2B; placed at 180° angel to each other. The satellites are located in the sun synchronous orbit about 786 Kms altitude from the earth surface [17]. A dedicated dual-frequency Global Navigation Satellite System (GNSS) tracks the position of both of the satellites in the orbit and accuracy is maintained using specific propulsion system. The Multispectral Instrument (MSI) developed by Astrium SAS (France); collects sunlight reflected from the Earth in order to maintain continuous observations [18-20]. This observational data is acquired at the instrument and referred as Level-0 products. The MSI instrument consists of two focal plane assemblies where incident light beam is split using filters. These focal planes are dedicated for two bands; one for Visible and Near-Infra-Red (VNIR) and other one for Short Wave Infra-Red (SWIR). The spectral separation of each band into individual wavelengths is accomplished by stripe filters mounted on top of the detectors. The swath width of the MSI telescope provides a 290 km Field of View (FOV). The schematic view of Sentinel-2 satellite has been described in Figure 2.

Figure 2: Schematic view of the deployed SENTINEL-2 spacecraft (image credit: EADS Astrium)

DATA AND METHODOLOGY

The recent eruption from Mt. Mayon has been analyzed using two stages. The 1st stage consists of processing Sentinel-2 images few days prior to the eruption and other image just after the eruption [21-24]. We have analyzed Sentinel-2 image acquired on 20th January 2018 as the day before eruption and image captured on 30th January 2018 as the day after eruption. Normalized Difference Vegetation Index (NDVI) has been processed in order to calculate change in pixel values of the same region of interest. This dedicated algorithm results the vegetation loss nearby the volcano by analyzing the change in pixel values. NDVI provides values ranging from -1 to +1 where +1 leads to the maximum change in pixels and -1 provides minimal changes [25]. The 2nd stage comprise of processing physical and optical properties of the erupted particles and SO2. Particles mass concentration, deposition and dispersion along with particles vertical position has also been studied from surface to 1000 Meters, 1000-2000 Meters and 2000-2500 Meters. Particle's dynamics into atmosphere has been analyzed using NOAA's Hysplit Trajectory Model along with Hysplit volcanic ash dispersion model [26]. We have analysed daily averaged SO2 mass concentration products from NASA's Moderate Resolution Imaging Spectroradiometer (MODIS) instrument. MODIS instrument is onboard Terra and Aqua satellites that monitors land, ocean and lower atmosphere [27]. Due to timed orbital propagation, both of the satellites revisit entire Earth's surface every 1-2 days. MODIS instrument uses 36 different wavelengths to generate various scientific products for land, ocean and atmospheric relevance [28]. These datasets are fruitful for improved understanding of global dynamics and environment. The vast range of MODIS products are helping researchers and policy makers to study the historical trend of Earth's environment in order to make decisions to control climate change globally [29].

RESULTS AND DISCUSSION

NDVI (Normalized Difference Vegetation Index)

NDVI is an algorithm to determine the density of green on a patch of land by observing the distinct wavelengths reflected by the plants over visible and NIR bands [30]. When the incident sunlight strikes an object; it absorbs some of the wavelengths of this spectrum and other wavelengths are reflected back to the space [31]. Chlorophyll in plant leaves strongly absorbs visible light 117 (from 0.4 to 0.7 µm) to use in photosynthesis process and cell structure of the leaves reflects NIR light (from 0.7 to 1.1 µm). The more leaves a plant has, the more these wavelengths of light are affected. Calculations of NDVI for a given pixel always result in a number that ranges from minus one (-1) to plus one (+1). NDVI value close to zero indicates the plants with no green leaves [32]. A zero means no vegetation and close to 1 (0.8-0.9) indicates the highest possible density of green leaves. NDVI algorithm calculates the ratio of differences in Near Infrared band (NIR) and visible band (VIS) to the total reflection from the surface.

NDVI = (NIR – VIS) / (NIR + VIS)

We have studied Satellite images from Sentinel-2 mission acquired on 20th January 2018 and 30th January 2018 for same subset area of interest. We have used B8 as NIR band and B4 as visible Red band from the image. The results show huge change in vegetation after the eruption in southwest direction of the volcano [33]. Pixel densities of dark Red pixels have proved the vegetation loss near volcano after the eruption. The mean pixel density of Dark red pixels has been observed 0.3595 after the eruption which was observed 0.1333 before the eruption [34]. The minimum value of NDVI has been observed -0.096 after the eruption which proves the existence of minimal or nearly no vegetation. Figure 3 describes the change in vegetation near the volcano.

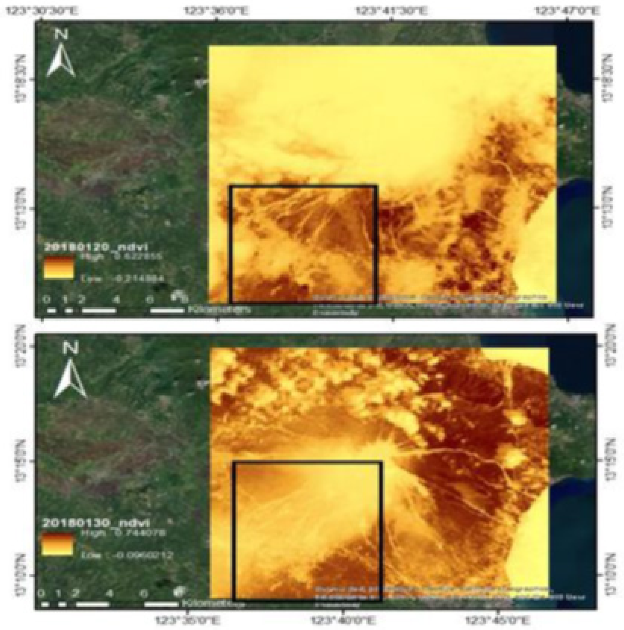

Figure 3: Change in NDVI

The image above comprise of comparison between two different sentinel images acquired on 20th January 2018 and 30th January 2018 respectively. High NDVI values represent higher vegetation near volcano and coded as dark Brown color. The box represents the highest change in NDVI and might be the slope of lava flow [35]. We have resampled the image at 20 meters resolution in order to get more accurate results. The total error has been calculated as 0.0008% in Sentinel-2 retrieved images which leads to the accuracy of the results. Table 1 below describes the statistics of the image analysis.

Table 1: Inter-comparison statistics using Sentinel-2 images.

Parameter	Before Eruption	After Eruption
Total No. of Pixels	110208	110208
Min	-0.2149	-0.096
Max	0.6229	0.7441
Mean	0.1333	0.3595
Sigma	0.1528	0.1930
Median	0.0884	0.3744
Coefficient Variation	1.3755	0.8342
Equivalent No. of Looks	0.5286	1.4369
Max Error	0.00083	0.00084

Mineral dust column mass density

Volcanic ash is formed by fragmentation process of the magma and the surrounding rock materials of volcanic vents. The released volcanic ash solely depends on the strength of the eruption. These ash clouds are transported by prevailing winds until the removal of the erupted particles from the atmosphere by wet deposition or gravitational settling. The mineral dust in the form of Particulate matter affects the radiative forcing of the atmosphere directly or indirectly by cloud condensation or ice nuclei [36]. Particle size in the mineral dust varies from 1 micrometer to 100 micrometer diameter. The coarser the particles, the faster they deposited. Dust column mass density has been analyzed as area averaged mass concentration over Mt. Mayon volcano. The results show a strong agreement with deposition of particles on 29th January 2018 with mass concentration of 0.000004 Kg/M2 [37]. A strong peak with particle deposition of 0.000008 Kg/M2 has also been observed on 31st January 2018. The area averaged mass concentration of erupted particles is described in Figure 4 below:

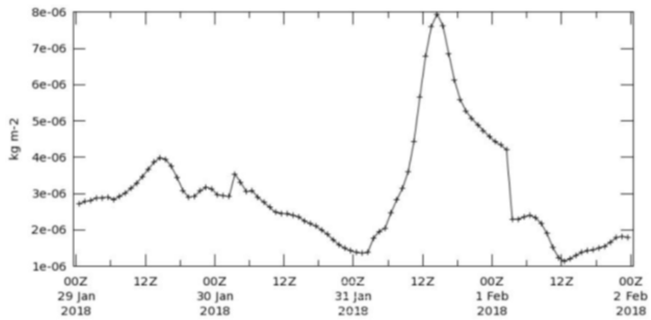

Figure 4: Mineral dust column mass density near Mt. Mayon

Sulfur dioxide (SO2) mass concentration

SO2 is one of the most concerning pollutants emitted by volcano that affects atmosphere by forming sulfate aerosols. SO2 Mass concentration has been observed from 29th Jan 2018 to 1st Feb 2018 in order to study the changes in SO2 amount near the volcano [38]. The results state that SO2 concentration has been observed 1.7 DU on 30th January and a dominant rise of 6.14% SO2 has also been observed on 31st January 2018 with concentration of 7.12 DU. Figure 5 describes SO2 mass concentration near the volcano.

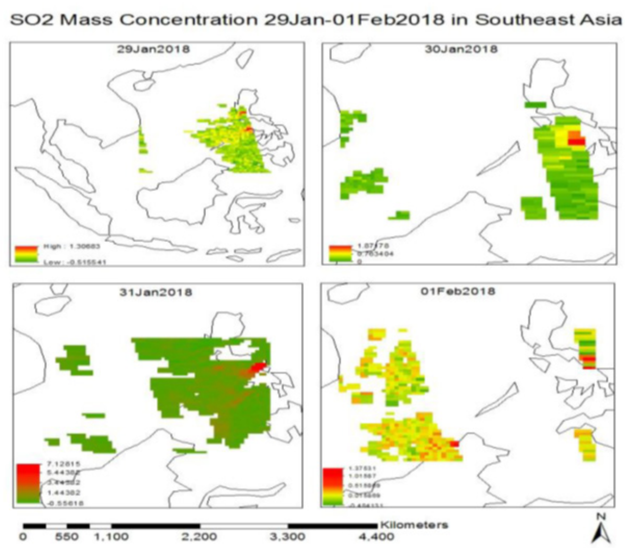

Figure 5: SO2 mass concentration near Mt. Mayon

Forward trajectory of airmass

Forward Trajectory of airmass has been calculated using NOAA's Hysplit trajectory model up to 72 Hours from the eruption [37]. The airmass flow has been calculated at three different above ground level height (AGL) 500 Meters, 2000 Meters and 2500 Meters. The trajectory shows that outbound winds starting from volcano travelled till Sarawak province of Malaysia in 72 Hours. The trajectory has been calculated using GFS model that provides up to 192 Hours forecast. Figure 6 describes forward trajectory of airmass from the source of eruption.

Figure 6: Forward trajectory of airmass

Particles deposition, dispersion and concentration

The setteling time of the aerosol particles varies with the size of the particles and the atmospheric conditions. During winters particles have lesser dispersive conditions as compared to that during summer. In present case; the emitted particles are deposited nearby the volcano and to study this effect we have used Hysplit Volcanic Ash Dispersion model [39]. The model uses global meteorological data provided by Air Resources Laboratory, USA and Real time environment application display system to study particles deposition near the source. The deposition time is within 24 Hrs of eruption. Model results have been described in Figure 7 as contour plots.

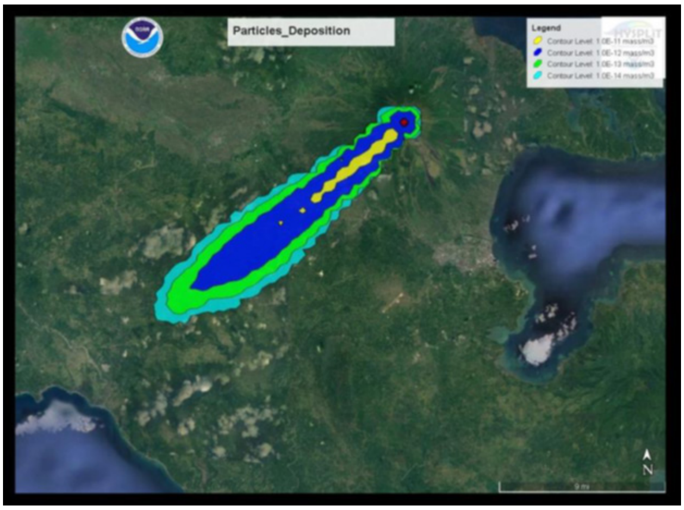

Figure 7: Particles deposition on 30.01.2018

Deposition of particles indicates that within 24 Hrs of eruption; particles transportation was up to a small geographic area near the volcano as meteorological condition were not much familiar for dispersion of particles. This is due to reduced settling velocity of particles by gaining increased mass as enhanced SO2 has been observed after eruption. After 24 Hrs of eruption; Hysplit model results that higher wind speed was observed at 1000-4000 Meters AGL that is responsible for dispersion of erupted particles [40]. These particles were carried by 1000-4000 Meters AGL winds up to coastal part of Sarawak, Malaysia. The results clearly show that within 72 Hrs of eruption; the highest mass concentration of volcanic particles has been observed from surface to 2000 Meters AGL. The results are represented in Figure 8 (a and b), Figure 9 below.

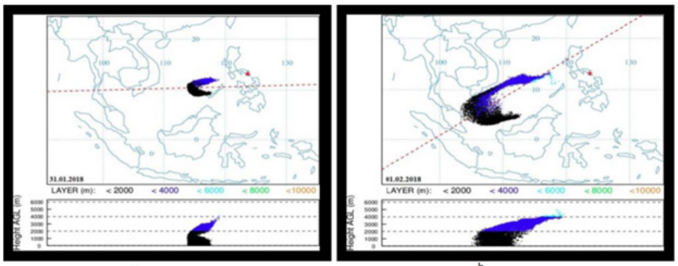

a b

Figure 8: (a): Particles dispersion on 31.01.2018. (b): Particles dispersion on 01.02.2018.

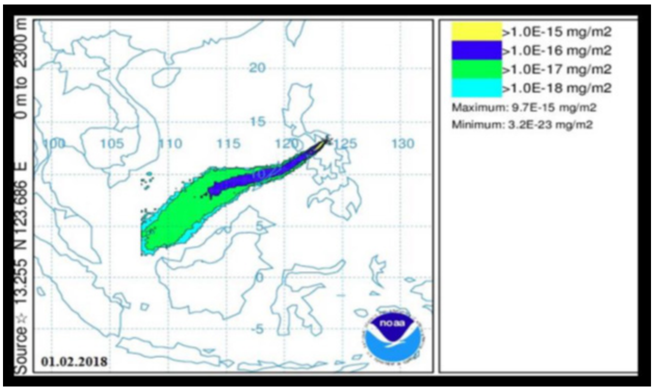

Figure 9: Deposition of particles on 01.02.2018.

SO2column mass density over sarawak

Area averaged SO2 mass concentration has shown increased SO2 amount near the volcano on 31st Jan 2018 and airmass trajectories show that the erupted particles were transported from Mt. Mayon to Northern Sarawak in 72 Hours. These particles resulted in increased SO2 concentration over Sarawak [41]. In order to validate our results, we have performed pixel-wise analysis of SO2 column mass density over Northern Sarawak from 01 Feb 2018 to 04 Feb 2018 using NASA's latest reanalysis method Merra-2 model hourly data. MERRA-2 uses latest version of GEOS-5 (Goddard Earth Observation System version-5) which is able to use the newer microwave sounders and hyper spectral infrared radiance instruments as well as other data types [42]. The MERRA-2 observing system is described by McCarty et al. Merra-2 data is sampled at 0.5º*0.625º grid which has been resampled at 0.5º*0.5º grid in order to equalize the cell area. These hourly averaged products have been aggregated to daily averaged products in order to demonstrate daily impact of incoming airmass. The results prove strong agreement with outbound wind pattern from the volcano and sudden increased SO2 on 04th Feb 2018. Results have been represented in Figure 10 below.

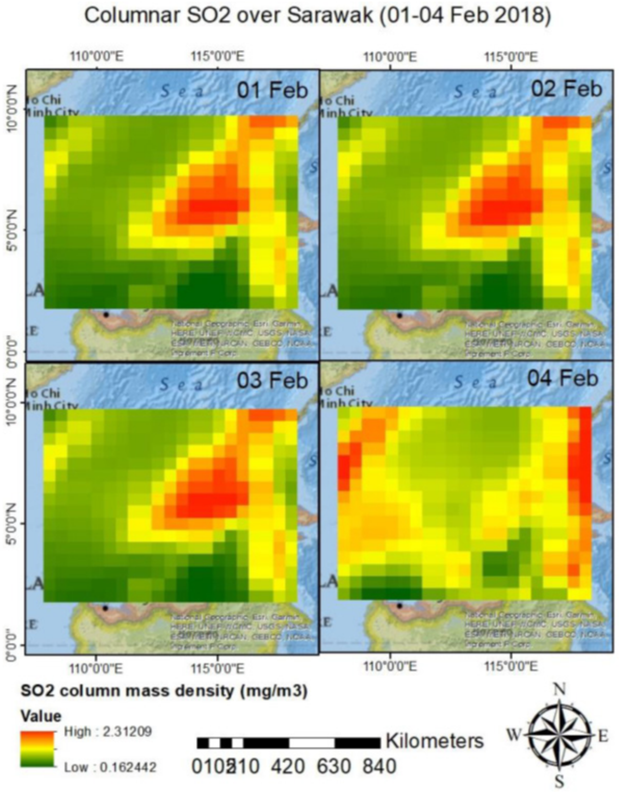

Figure 10: SO2 column mass density over Sarawak after 31st Jan 2018.

CONCLUSION

The eruption at Mt. Mayon affected the environment of a huge part of Southeast Asia. The mass concentration of erupted SO2 was observed till Malaysia from Philippines. Outbound winds from the point of eruption carried a huge amount of erupted particles. These particles have been found in the atmosphere after a week of eruption. The case study shows that the maximum concentration of SO2 was found 2.31209 mg/m3 over Sarawak after three days of eruption which exerted sudden increase on 4th Feb 2018. This much concentration of SO2 is harmful as it irritates the nose, throat, and airways to cause coughing, wheezing, shortness of breath, or a tight feeling around the chest. The effects of sulfur dioxide are felt very quickly and most people would feel the worst symptoms in 10 or 15 minutes after breathing it in. The future research work needs more stable monitoring of volcanic eruption and need to develop an effective approach to reduce its effects over environment as well as public health.

REFERENCES

1. Allen AG, Oppenheimer C, Ferm M, Baxter PJ, Horrocks L A, Galle B, et.al. Plume velocity determination for volcanic SO2 flux measurements. Geophys Res Lett. 2004;109(21): 1–17.
2. Aiuppa A, Inguaggiato S, McGonigle AJS, O'Dwyer M, Oppenheimer C, Padgett MJ, et al. H 2 S fluxes from Mt. Etna, Stromboli, and Vulcano (Italy) and 390 implications for the sulfur budget at volcanoes. Geochimica et Cosmochimica Acta. 2005;69(7): 1861–1871.
3. Cigolini C, Borgia A, Casertano L. Intra-crater activity, aa-block lava, viscosity and flow dynamics: Arenal Volcano, Costa Rica. J Vol Geo Research. 1984;20(1–2): 274 155–176.
4. Dare R. Sedimentation of volcanic ash in the HYSPLIT dispersion model. In CAWCR Technical Report No. 2015;079.
5. Matasci G, Longbotham N, Pacifici F, Kanevski M, Tuia D. Understanding angular effects in VHR imagery and their significance for urban land-cover model portability: A study of two multi-angle in-track image sequences. ISPRS. 2015
6. Carlson TN, Ripley DA. On the relation between NDVI, fractional vegetation cover, and leaf area index. Remote Sensing of Environment.1997
7. Xu Z, Wang X, Chen Z, Xiong D, Ding M Hou W. Nonlocal similarity based DEM 315 super resolution. ISPRS.2 015
8. Sibanda M, Mutanga O, Rouget M. Examining the potential of Sentinel-2 MSI spectral resolution in quantifying above ground biomass across different fertilizer treatments. ISPRS. 2015;110: 55–65.
9. Wild M, Ohmura A, Schär C, Müller G, Folini D, Schwarz M, Zyta Hakuba M, Sanchez-Lorenzo A. The Global Energy Balance Archive (GEBA) version 2017: A database for worldwide measured surface energy fluxes. Earth Science. 2017;9(2): 601–613.
10. Glasow R Von, Bobrowski N, Kern C. The effects of volcanic eruptions on atmospheric chemistry. Chemical Geology. 2009;263(1–4): 131–142.
11. Kannan PS, Office M. Temporal variations and the effect of volcanic eruptions on atmospheric turbidity over India. Mausam. 2003;pp: 881–890.
12. Yassin MF, Al-Shatti LA, Al Rashidi MS. Assessment of the atmospheric mixing height and its effects on pollutant dispersion. Environ Monit Assess. 2018;190(7).
13. Murthy BS, Latha R, Tiwari A, Rathod A, Singh S, Beig G. Impact of mixing layer 283 height on air quality in winter. Science of The Total Environment. 2020;197.
14. Zerefos C, Nastos P, Balis D, Papayannis A, Kelepertsis A, Kannelopoulou E, et.al. A complex study of Etna's volcanic plume from ground-based, in situ and space-borne observations. International J Remote Sensing. 2006;27(9): 1855–1864.
15. Donlon C, Berruti B, Buongiorno A, Ferreira MH, Féménias P, Frerick J, et.al. The Global Monitoring for Environment and Security (GMES) Sentinel-3 mission. Remote Sens Environ. 2012;120: 37-57.
16. Drusch M, Del Bello U, Carlier S, Colin O, Fernandez V, Gascon F, et.al. Sentinel-2: ESA's optical high-resolution mission for GMES operational services. Remote Sens Environ. 2012;120: 25-36.
17. Wu Y, Zhao K, Huang J, Arend M, Gross B, Moshary F. Observation of heat wave effects on the urban air quality and PBL in New York City area. Atmos Environ. 2019;218.
18. Geiß A, Wiegner M, Bonn B, Schäfer K, Forkel R, Von Schneidemesser E, et.al. Mixing layer height as an indicator for urban air quality? Atmos Meas Tech. 2017;10(8): 2969–2988.
19. Tang G, Zhang J, Zhu X, Song T, Münkel C, Hu B, et.al. Mixing layer height and its implications for air pollution over Beijing, China. Atmos Chem Phys. 2016;16(4): 2459–2475.
20. Wu Y, Zhao K, Huang J, Arend M, Gross B, Moshary F. Observation of heat wave effects on the urban air quality and PBL in New York City area. Atmos Environ. 2019;218.
21. Zheng S, Singh RP, Wu Y, Wu C. A comparison of trace gases and particulate matter over Beijing (China) and Delhi (India). Water Air & Soil Pollution. 2017;228(5).
22. Chen Y, Wild O, Ryan E, Sahu SK, Lowe D, Archer-Nicholls S, et.al. Mitigation of PM2.5 and ozone pollution in Delhi: A sensitivity study during the pre-monsoon period. Atmos Chem Phys. 2019;20: 499-514.
23. Rückerl R, Schneider A, Breitner S, Cyrys J, Peters A. Health effects of particulate air pollution: A review of epidemiological evidence. Inhal Toxicol. 2011;23(10): 555–592.

24. Lelieveld J, Evans JS, Fnais M, Giannadaki D, Pozzer A. The contribution of outdoor air pollution sources to premature mortality on a global scale. Nature. 2015;525(7569): 367–371.

25. Dutrieux LP, Verbesselt J, Kooistra L, Herold M. Monitoring forest cover loss using multiple data streams, a case study of a tropical dry forest in Bolivia. ISPRS J Photogramm Remote Sens. 2015.

26. Kannan PS, Office M. Temporal variations and the effect of volcanic eruptions on atmospheric turbidity over India. 2003;pp: 881–890.

27. Seibert P, Beyrich F, Gryning SE, Joffre S, Rasmussen A, Tercier P. Review and intercomparison of operational methods for the determination of the mixing height. Atmos Environ. 2000;34(7): 1001–1027.

28. Pinedo JL, Mireles-García F, Rios C, García-Saldivar VM, Ignacio Davila-Rangel J, Espinosa JR. Assessment of the latitudinal behavior of total column Ozone at nine discrete 1° wide latitude bands, from TOMS and OMI Data. Open Atmospheric Science Journal. 2013;7(1): 92–109.

29. Jiang Z, Huete AR, Chen J, Chen Y, Li J, Yan G, et al. Analysis of NDVI and scaled difference vegetation index retrievals of vegetation fraction. Remote Sens Environ. 2006;101(3): 366-378.

30. Charron A, Harrison RM. Atmospheric nanoparticles. Jamie R, Emma S. Environmental and human health impacts of nanotechnology. 2009.

31. Moses WJ, Sterckx S, Montes MJ, De Keukelaere L, Knaeps E. Atmospheric correction for Inland waters. In bio-optical modeling and remote sensing of inland waters. 2017.

32. Hartmann DL, Klein Tank AMG, Rusticucci M, Alexander LV, Brönnimann S, Charabi YAR, et al. Observations: Atmosphere and surface. In climate change 2013 the physical science basis: Working group I contribution to the fifth assessment report of the intergovernmental panel on climate change 2013.

33. Austin J, Tourpali K, Rozanov E, Akiyoshi H, Bekki S, Bodeker G, et al. Coupled chemistry climate model simulations of the solar cycle in ozone and temperature. J Geo Research Atmospheres. 2018;113(11): 1–20.

34. Pöschl U. Atmospheric chemistry atmospheric aerosols: Composition, transformation, climate and health effects. Angewandte. 2005;44(46): 7520–7540.

35. Stenchikov G, Kirchner I. Radiative forcing from the 1991 Mount Pinatubo volcanic eruption. 2015.

36. Poulidis AP, Takemi T, Shimizu A, Iguchi M, Jenkins SF. Statistical analysis of dispersal and deposition patterns of volcanic emissions from Mt . Sakurajima , Japan. Atmospheric Environment. 2018;179: 305–320.

37. Iii CAP, Dockery DW. 381 Health effects of fine particulate air pollution: Lines that Connect. J Air Waste Manag Assoc. 2012;56(6): 709-742.

38. Sellitto P, Zanetel C, Salerno G, Tapparo A, Meloni D, Pace G, et al. The impact of Mount Etna sulfur emissions on the atmospheric composition and aerosol properties in the central Mediterranean : A statistical analysis over the period 2000 e 2013 based on observations and Lagrangian modelling. Atmos Environ. 2017;148(1): 77–88.

39. Chai T, Crawford A, Stunder B, Pavolonis MJ, Draxler R, Stein A. Improving volcanic ash predictions with the HYSPLIT dispersion model by assimilating MODIS satellite retrievals. Atmos Chem Phys. 2017;17: 2865–2879.

40. McGonigle AJS, Hilton DR, Fischer TP, Oppenheimer C. Plume velocity determination for volcanic SO2 flux measurements. Geophys Res Lett. 2005;32(11): 1–4.

41. Loyola D, Van Geffen J, Valks P, Erbertseder T, Van Roozendael M, Thomas W, et al. Satellite-based detection of volcanic sulphur dioxide from recent eruptions in Central and South America. Advances in Geosciences, 2008;14: 35–40.

42. Antuna JC, Graf HF, Grainger RG, Kirchner I, Lambert A, Robock A, et al. Radiative forcing from the 1991 Mount Pinatubo volcanic eruption. J Geo Research-Atmospheres. 1998;103(D12): 13837-13857.